Fatigue evaluation in maintenance and assembly operations by digital human simulation

Liang MA · **Damien CHABLAT** · **Fouad BENNIS** · **Wei ZHANG** · **Bo HU** ·
François GUILLAUME

Abstract Virtual human techniques have been used a lot in industrial design in order to consider human factors and ergonomics as early as possible. The physical status (the physical capacity of virtual human) has been mostly treated as invariable in the current available human simulation tools, while indeed the physical capacity varies along time in an operation and the change of the physical capacity depends on the history of the work as well. Virtual Human Status is proposed in this paper in order to assess the difficulty of manual handling operations, especially from the physical perspective. The decrease of the physical capacity before and after an operation is used as an index to indicate the work difficulty. The reduction of physical strength is simulated in a theoretical approach on the basis of a fatigue model in which fatigue resistances of different muscle groups were regressed from 24 existing maximum endurance time (MET) models. A framework based on digital human modeling technique is established to realize the comparison of physical status. An assembly case in airplane assembly is simulated and analyzed under the framework. The endurance time and the decrease of the joint moment strengths are simulated. The experimental result in simu-

Liang MA · Damien CHABLAT · Fouad BENNIS
Institut de Recherche en Communications et Cybernétique de Nantes, UMR 6597 du CNRS, École Centrale de Nantes, IRCCyN - 1, rue de la Noë - BP 92 101 - 44321 Nantes CEDEX 03, FRANCE
Tel.:+33-02 40 37 69 58
Fax: +33-02 40 37 69 30
E-mail: {liang.ma, damien.chablat, fouad.bennis}@irccyn.ec-nantes.fr

Wei ZHANG · Bo HU
Department of Industrial Engineering, Tsinghua University, 100084, Beijing, P.R.CHINA
E-mail: zhangwei@tsinghua.edu.cn, b-hu05@mails.tsinghua.edu.cn

François GUILLAUME
EADS Innovation Works, 12, rue Pasteur - BP 76, 92152 Suresnes Cedex - FRANCE
E-mail: francois.guillaume@eads.net

lated operations under laboratory conditions confirms the feasibility of the theoretical approach.

1 Introduction

Although automation techniques have played a very important role in industry, there are still lots of operations requiring manual handling operations thanks to the flexibility and the dexterity of human. Some of these manual handling operations deal with relative heavy physical loads, which might result in physical fatigue in the muscles and joints, and further generate potential risks for Musculoskeletal Disorders (MSDs) (Li and Buckle, 1999).

In order to improve the work design, digital human modeling (DHM) technique has been used more and more in industry taking human as the center of the work design system (Chaffin, 2002, 2007), since it benefits the validation of the workspace design, the assessment of the accessibility of an assembly design, the reduction of the production cost, and the reduction of the physical risks as well.

Several commercial available DHM tools have already been developed and integrated into computer aided design (CAD) tools, such as Jack (Badler et al, 1993), 3DSSPP (Chaffin et al, 1999), RAMSIS (Bubb et al, 2006), AnyBody (Damsgaard et al, 2006), Santos^{TM} (VSR Research Group, 2004), etc. In general, the virtual human in those tools is modeled with a large number of degrees of freedom (DOF) to represent the joint mobility, create the cinematic chain of human, and complete the skeleton structure of human. Meanwhile, the graphical appearance of virtual human is realized by bone, muscle, skin, and cloth models from the interior to the exterior, from simple stick models to complicated 3D mesh models. Normally, biomechanical database and anthropometry database

are often set up to determine virtual human's dimensional and physical properties.

The main functions of the virtual human simulation tools are posture analysis and posture prediction. These tools are capable of determining the workspace of virtual human (Yang et al, 2008), assessing the visibility and accessibility of an operation (Chedmail et al, 2003), evaluating postures (Bubb et al, 2006), etc. Conventional motion time methods (MTM) and posture analysis techniques can be integrated into virtual human simulation systems to assess the work efficiency (Hou et al, 2007). From the physical aspect, the moment load of each joint (e.g., 3DSSPP) and even the force of each individual muscle (e.g., AnyBody) can be determined, and the posture is predictable for reach operations (Yang et al, 2006) based on inverse kinematics and optimization methods. Overall, the human motion can be simulated and analyzed based on the workspace information, virtual human strength information, and other aspects. However, there are still several limitations in the existing virtual human simulation tools.

There is no integration of physical fatigue model in most of the human simulation tools. The physical capacity is often initialized as constant. For example, the joint strength is assigned as joint maximum moment strength in 3DSSPP, and the strength of each muscle is set proportional to its physiological cross section area (PSCA) in AnyBody. The physical capacity keeps constant in the simulation, and the fatigue effect along time is not considered enough. However, the change of the physical status can be experienced everyday by everyone, and different working procedures generate different fatigue effects. Furthermore, it has been reported that the motion strategy depends on the physical status, and different strategies were taken under fatigue and non-fatigue conditions (Chen, 2000; Fuller et al, 2008). Therefore, it is necessary to create a virtual human model with a variable physical status for the simulation.

Some fatigue models have been incorporated into some virtual human tools to predict the variable physical strength. For example, Wexler's fatigue model (Ding et al, 2000) has been integrated into Santos^{TM} (Vignes, 2004), and Giat's fatigue model (Giat et al, 1993) has been integrated based on Hill's muscle model (Hill, 1938) in the computer simulation by Komura et al (2000). However, either the muscle fatigue model has too many variables for ergonomic applications (e.g. Wexler's model), or there is no confidential physiological principle for the fatigue decay term (Xia and Frey Law, 2008) in the previous studies. It is necessary to find a simple fatigue model interpretable in muscle physiological mechanism for ergonomics applications.

In addition, some assessments in those tools provide indexes generated by traditional evaluation methods (e.g., Rapid upper limb assessment (RULA)). Due to the intermittent recording procedures of the conventional posture analysis methods, the evaluation result cannot analyze the fatigue effect

in details. In this case, a new fatigue evaluation tool should be developed and integrated into virtual human simulation.

In order to assess the variable human status, a prototype of a digital human modeling and simulation tool developed in OpenGL is presented in this paper. This human modeling tool is under a virtual environment framework involving variable physical status on the basis of a fatigue model.

The structure of the paper is as follows. First, a virtual human model is introduced into the framework for posture analysis based on kinematic, dynamic, biomechanical, and graphical modeling. Second, the framework is presented with a new definition called Human Status. Third, the fatigue model and fatigue resistance for different muscle groups are introduced. At last, an application case European Aeronautic Defence & Space (EADS) Company is assessed using this prototype tool under the framework with experimental validation.

2 Digital human modeling

2.1 Kinematic modeling of virtual human

In this study, the human body is modeled kinematically as a series of revolute joints. The Modified Denavit-Hartenberg (modified DH) notation system (Khalil and Dombre, 2002) is used to describe the movement flexibility of each joint. According to the joint function, one natural joint can be decomposed into 1 to 3 revolute joints. Each revolute joint has its rotational joint coordinate, labeled as q_i, with joint limits: the upper limit q_i^U and the lower limit q_i^L. A general coordinate $\mathbf{q} = [q_1, q_2, \ldots, q_n]$ is defined to represent the kinematic chain of the skeleton.

The human body is geometrically modeled by 28 revolute joints to represent the main movement of the human body in Fig. 1. The posture, velocity, and acceleration are expressed by the general coordinates $\mathbf{q}$, $\dot{\mathbf{q}}$, and $\ddot{\mathbf{q}}$. It is feasible to carry out the kinematic analysis of the virtual human based on this kinematic model. By implementing inverse kinematic algorithms, it is able to predict the posture and trajectory of the human, particularly for the end effectors (e.g., the hands). All the parameters for modeling the virtual human are listed in Table 1. $[X_r, Y_r, Z_r]$ is the Cartesian coordinates of the root point (the geometrical center of the pelvis) in the coordinates defined by $X_0Y_0Z_0$.

The geometrical parameters of the limb are required in order to accomplish the kinematic modeling. Such information can be obtained from anthropometry database in the literature. The dimensional information can also be used for the dynamic model of the virtual human. The lengths of different segments can be calculated as a proportion of body stature H in Table 2.

Table 1 Geometric modeling parameters of the overall human body

j	$a(j)$	u_j	σ_j	γ_j	b_j	α_j	d_j	q_j	r_j	q_{ini}
1	0	1	0	0	Z_r	$-\frac{\pi}{2}$	X_r	θ_1	Y_r	0
2	1	0	0	0	0	$\frac{\pi}{2}$	0	θ_2	0	$\frac{\pi}{2}$
3	2	0	0	0	0	$\frac{\pi}{2}$	0	θ_3	0	$\frac{\pi}{2}$
4	3	0	0	0	0	$\frac{\pi}{2}$	0	θ_4	R_{lb}	0
5	4	0	0	0	0	$-\frac{\pi}{2}$	0	θ_5	0	0
6	5	0	0	0	0	$\frac{\pi}{2}$	0	θ_6	R_{ub}	$\frac{\pi}{2}$
7	6	0	0	0	0	$\frac{\pi}{2}$	0	θ_7	0	0
8	7	0	0	0	0	$\frac{\pi}{2}$	0	θ_8	0	0
9	5	1	0	$-\frac{\pi}{2}$	0	0	D_{ub}	θ_9	$-\frac{W_s}{2}$	0
10	9	0	0	0	0	$-\frac{\pi}{2}$	0	θ_{10}	0	$-\frac{\pi}{2}$
11	10	0	0	0	0	$-\frac{\pi}{2}$	0	θ_{11}	$-R_{ua}$	$-\frac{\pi}{2}$
12	10	0	0	0	0	$-\frac{\pi}{2}$	0	θ_{12}	0	0
13	11	0	0	0	0	$\frac{\pi}{2}$	0	θ_{13}	0	0
14	5	1	0	$-\frac{\pi}{2}$	0	0	D_{ub}	θ_{14}	$\frac{W_s}{2}$	0
15	14	0	0	0	0	$-\frac{\pi}{2}$	0	θ_{15}	0	$-\frac{\pi}{2}$
16	15	0	0	0	0	$-\frac{\pi}{2}$	0	θ_{16}	$-R_{ua}$	$-\frac{\pi}{2}$
17	16	0	0	0	0	$-\frac{\pi}{2}$	0	θ_{17}	0	0
18	17	0	0	0	0	$\frac{\pi}{2}$	0	θ_{18}	0	0
19	1	1	0	$-\frac{\pi}{2}$	0	$-\frac{\pi}{2}$	0	θ_{19}	$-\frac{W_w}{2}$	$-\frac{\pi}{2}$
20	19	0	0	0	0	$-\frac{\pi}{2}$	0	θ_{20}	0	$-\frac{\pi}{2}$
21	20	0	0	0	0	$-\frac{\pi}{2}$	0	θ_{21}	$-R_{ul}$	$-\frac{\pi}{2}$
22	21	0	0	0	0	$-\frac{\pi}{2}$	0	θ_{22}	0	$-\frac{\pi}{2}$
23	22	0	0	0	0	0	$-D_{ll}$	θ_{23}	0	0
24	1	1	0	$-\frac{\pi}{2}$	0	$-\frac{\pi}{2}$	0	θ_{24}	$\frac{W_w}{2}$	$-\frac{\pi}{2}$
25	24	0	0	0	0	$-\frac{\pi}{2}$	0	θ_{25}	0	$-\frac{\pi}{2}$
26	25	0	0	0	0	$-\frac{\pi}{2}$	0	θ_{26}	$-R_{ul}$	$-\frac{\pi}{2}$
27	26	0	0	0	0	$-\frac{\pi}{2}$	0	θ_{27}	0	$-\frac{\pi}{2}$
28	27	0	0	0	0	0	$-D_{ll}$	θ_{28}	0	0

Table 2 Body segment lengths as a proportion of body stature (Chaffin et al, 1999; Tilley and Dreyfuss, 2002)

Symbol	Segment	Length
R_{ua}	Upper arm	0.186H
R_{la}	Forearm	0.146H
R_h	Hand	0.108H
R_{ul}	Thigh	0.245H
D_{ll}	Shank	0.246H
W_s	Shoulder width	0.204H
W_w	Waist width	0.100H
D_{ub}, L_{ub}	Torso length (L5-L1)	0.198H
R_{ub}	Torso length (L1-T1)	0.090H

Table 3 Percentage distribution of total body weight according to different segmentation plans (Chaffin et al, 1999)

Grouped segments, % of total body weight	individual segments % of grouped-segments weight
Head and neck=8.4%	Head=73.8%
	Neck=26.2%
Torso=50%	Thorax=43.8%
	Lumbar=29.4%
	Pelvis=26.8%
Total arm=5.1%	Upper Arm=54.9%
	Forearm=33.3%
	Hand=11.8%
Total leg=15.7%	Thigh=63.7%
	Thigh=63.7%
	Shank=27.4%
	Foot=8.9%

2.2 Dynamic modeling of virtual human

Necessary dynamic parameters for each body segment include: gravity center, mass, moment of inertia about the gravity center, etc. According to the percentage distribution of total body weight for different segments (Chaffin et al, 1999), the weights of different segments can be calculated using Table 3.

It is feasible to calculate other necessary dynamic information with simplification of the segment shape. For limbs, the shape is simplified as a cylinder, head as a ball, and torso as a cube. The moment of inertia can be further determined based on the assumption of uniform density distribution. For the virtual human system, once all the dynamic parameters are known, it is possible to calculate the torques and forces at each joint following Newton-Euler method (Khalil and Dombre, 2002).

2.3 Biomechanical modeling of virtual human

The biomechanical properties of the musculoskeletal system should also be modeled for virtual human simulation. From
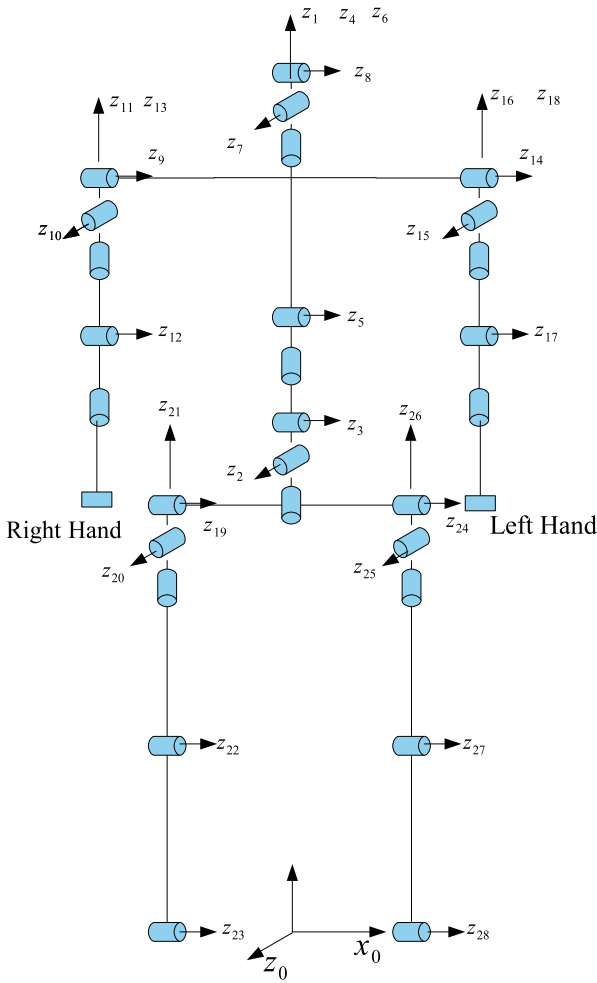
Fig. 1 Geometrical modeling of virtual human

The joint torque capacity is the overall performance of muscles attached around the joint, and it depends on the posture and the rotation speed of joint (Anderson et al, 2007). When a heavy load is handled in a manual operation, the action speed is relatively small, and it is almost equivalent to static cases. The influence from speed can be neglected, so only posture is considered. In this situation, the joint strength can be determined according to strength models in Chaffin et al (1999). The joint strength is measured in torque and modeled as a function of joint flexion angles. An example of joint strength is given in Fig. 2. The shoulder flexion angle and the elbow flexion angle are used to determine the profile of the male adult elbow joint strength. The 3D mesh surfaces represent the elbow joint strengths for 95% population. For the 50th percentile, the elbow joint strength varies from 45 to 75 N according to the joint positions.
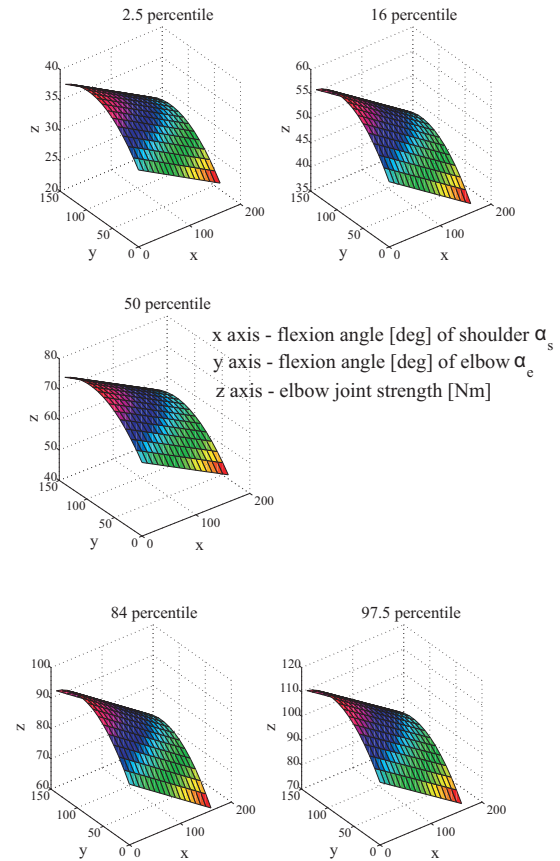
the physical aspect, the skeleton structure, muscle, and joint are the main biomechanical components in a human. In our study, only the joint moment strengths and joint movement ranges are used for the fatigue evaluation.

As mentioned before, with correct kinematic and dynamic models, it is possible to calculate torques and forces in joints with an acceptable precision. Although biomechanical properties of muscles are reachable and different optimization methods have been developed in the literature, the determination of the individual muscle force is still very complex and not as precise as that of joint torque (Xia and Frey Law 2008). Since there are several muscles attached around a joint, it creates an mathematical underdetermined problem for force calculation in muscle level. In addition, each individual muscle has different muscle fiber compositions, different levers of force, and furthermore different muscle coordination mechanisms, and the complexity of the problem will be increased dramatically in muscle level. Therefore, in our system, only the joint moment strength is taken to demonstrate the fatigue model.

x axis - flexion angle [deg] of shoulder α_s
y axis - flexion angle [deg] of elbow α_e
z axis - elbow joint strength [Nm]

Fig. 2 Elbow static strength depending on the human elbow and shoulder joint position, α_s, α_e [deg]

2.4 Graphical modeling of virtual human

The final step for modeling the virtual human is its graphical representation. The skeleton is divided into 11 segments: body (1), head and neck (1), upper arms (2), lower arms (2), upper legs (2), lower legs (2), and feet (2). Each segment is modeled in 3ds file (3D Max, Autodesk Inc.) (Fig. 3(a)) and is connected via one or more revolute joints with another one to assemble the virtual skeleton (Fig. 3(b)). For each segment, an original point and two vectors perpendicular to each other are attached to it to represent the position and the orientation in the simulation, respectively. The position and orientation can be calculated by the kinematic model of the virtual human.

(a) 3DS model   (b) virtual skeleton
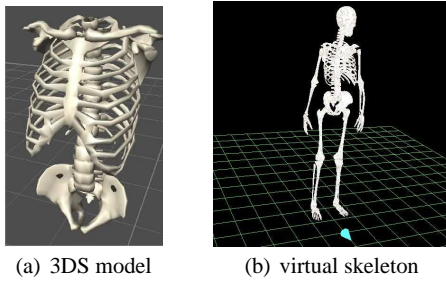
Fig. 3 Virtual skeleton composed of 3DS models

3 Framework for evaluating manual handling operations

The center of the framework is the objective work evaluation system (OWES) in Fig. 4. The input module includes: human motion, interaction information, and virtual environment. Human motion is either captured by motion capture system or simulated by virtual human simulation. The interaction information is either obtained via haptic interfaces or modeled in simulation. Virtual environment is constructed to provide visual feedback to participants or workspace information in simulation. Input information is processed in OWES. With different evaluation criteria, different aspects of human work can be assessed as in the previous human simulation tools.

A new conception **human status** is proposed for this framework to generalize the discussion. **Human Status**: it is a state, or a situation in which the human possesses different capacities for an industrial operation. It can be further classified into mental status and physical status. Human status can be described as an aggregation of a set of human abilities, such as visibility, physical capacity (joint strength, muscle strength), and mental capacity. Virtual human status can be mathematically noted as $\mathbf{HS} = \{\mathbf{V}_1, \mathbf{V}_2, \ldots, \mathbf{V}_n\}$. Each $\mathbf{V}_i$ represents one specific aspect of human abilities,
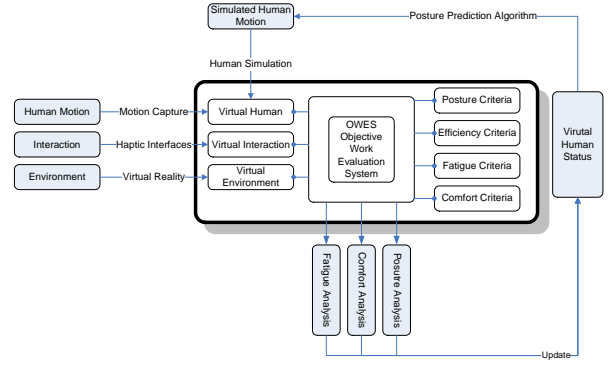
Fig. 4 Framework for the work evaluation

and this state vector can be further detailed by a vector $\mathbf{V}_i = \{v_{i1}, v_{i2}, \ldots, v_{im_i}\}$. The change of the human status is defined as $\Delta\mathbf{HS} = \mathbf{HS}(t + \delta t) - \mathbf{HS}(t) = \{\Delta\mathbf{V}_1, \Delta\mathbf{V}_2, \ldots, \Delta\mathbf{V}_n\}$. For example, one aspect of the physical status can be noted as $\mathbf{HS} = [S_1, S_2, \ldots, S_n]$, where S_i represents the physical joint strength of the ith joint of the virtual human.

In order to make the simulation as realistic as in real world, it is necessary to know how the human generates a movement. The bidirectional communication between human and the real world in an operation decides the action to accomplish a physical task: worker's mental and physical status can be influenced by the history of operation, while the worker chooses his or her suitable movement according to his or her current mental and physical statuses. Hence the framework is designed to evaluate the change of human status before and after an operation, and furthermore to predict the human motion according to the changed human status.

The human is often simplified for posture control as a sensory-motor system in which there are enormous external sensors covering the human body and internal sensors in the human body capturing different signals, and the central nervous system (CNS) transfer the signals into decision making system (Cerebrum and Vertebral disc); the decision making system generates output commands to generate forces in muscles and then drives the motion and posture responding to the external stimulus. Normally, most of the external input information is directly measurable, such as temperature, external load, moisture, etc. However, how to achieve all the information for such a great number of sensors all over the human body is a challenging task. In addition, the internal perception of human body, which plays also an important role in motor sensor coordination, is much more difficult to be quantified. The most difficult issue is to know how the brain handles all the input and output signals while performing a manual operation. In previous simulation tools, the external input information has been already provided and handled. Visual feedback, audio feedback, and haptic feedback are often employed as input channel for a virtual human simulation. One limitation of the existing methods is that the in-

ternal sensation is not considered enough. Physical fatigue is going to be modeled and integrated into the framework to predict the perceived strength reduction and the reactions of the human body to the fatigue, which provides a close-loop for the human simulation (Fig. 5).
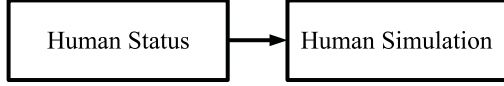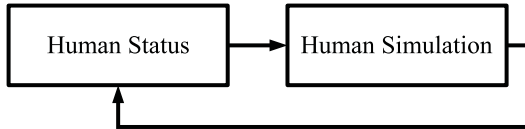

Fig. 5 Human status in human simulation tools

The special contribution in this framework is that the reduction of the physical strength can be evaluated in the framework based on a muscle fatigue model. And then the changed physical strength is taken as a feedback to the virtual human simulation to update the simulation result.

The framework performs mainly two functions: posture analysis and posture prediction (human simulation). The function of posture prediction is to simulate the human motion based on the current virtual human status. Posture analysis focuses on assessing the difficulty of the manual operation. The difficulty of the work is assessed by the change of human status before and after the operation $\Delta \mathbf{HS} = \Delta \mathbf{HS}_{physical}$. Physical fatigue is one of the physical aspects, and this aspect is evaluated by the decrease of the strength in joints. The posture analysis function of the framework is our focus in this paper.

More precisely in this paper, the joint strengths models are used to determine the initial joint moment capacity, and then the fatigue in the joints can be further determined by the external load in the static operation and the fatigue model in Section 4, and then the change of the physical status can be assessed.

4 Fatigue modeling and Fatigue analysis

4.1 Fatigue modeling

A new dynamic fatigue model based on muscle motor unit recruitment principle was proposed in (Ma et al, 2009). This model was able to integrate task parameters (external load) and temporal parameters for predicting the fatigue of static manual handling operations in industry. Equation 1 is the original form of the fatigue model to describe the reduction

of the capacity. The descriptions of the parameters for Eq. 1 are listed in Table 4. The detailed explanation about this model can be found in Ma et al (2009).

$$\frac{dF_{cem}(t)}{dt} = -k \frac{F_{cem}(t)}{MVC} F_{load}(t) \qquad (1)$$

Table 4 Parameters in dynamic fatigue model

Item	Unit	Description
MVC	N	Maximum voluntary contraction, maximum capacity of muscle
$F_{cem}(t)$	N	Current exertable maximum force, current capacity of muscle
$F_{load}(t)$	N	External load of muscle, the force which the muscle needs to generate
k	min^{-1}	Constant value, fatigue ratio
$\%MVC$		Percentage of the voluntary maximum contraction
f_{MVC}		$\%MVC/100$, $\frac{F_{load}(t)}{MVC}$

Maximum endurance time (MET) models can be used to predict the endurance time of a static operation. In static cases, $F_{load}(t)$ is constant in the fatigue model, and then MET is the duration in which F_{cem} falls down to F_{load}. Thus, MET can be determined in Eq. (2) and (3).

$$F_{cem}(t) = MVC \, e^{\int_0^t -k \frac{F_{load}(u)}{MVC} du} = F_{load}(t) \qquad (2)$$

$$t = MET = -\frac{ln \frac{F_{load}(t)}{MVC}}{k \frac{F_{load}(t)}{MVC}} = -\frac{ln(f_{MVC})}{k f_{MVC}} \qquad (3)$$

This model was validated in comparison with 24 MET models summarized in El ahrache et al (2006). The previous MET models were used to predict the maximum endurance time for static exertions and they were all described in functions with f_{MVC} as the only variable. High Pearson's correlations and interclass correlations (ICC) between the MET model in Eq. 3 and the other previous MET models validated the availability of our model for static cases. Meanwhile, the comparison between our model and a dynamic motor unit recruitment based model (Liu et al, 2002) suggested that our model was also suitable for modeling muscle fatigue in dynamic cases.

In (Ma et al, 2009), the fatigue ratio k was assigned 1 min^{-1}. However, from the literature, substantial variability in fatigue resistance in the population, and the variability results from several factors, such as age, career, gender, muscle groups, etc. The parameter k can handle the effects on

the fatigue resistance globally. Therefore, it is necessary to determine the fatigue resistances for different muscle groups to complete the muscle fatigue model.

4.2 Fatigue resistance based on MET models

Thanks to the high linear relationship between our MET model and the previous MET models, it is proposed that each static MET model $f(x)$ can be described mathematically by a linear equation (Eq. 4). In Eq. 4, x is used to replace f_{MVC} and $p(x)$ represents Eq. 3. m and n are constants describing the linear relationship between static model and our model, and they need be determined in regression. Here, $m = 1/k$ indicates the fatigue resistance of the static model, and k is fatigue ratio or fatigability of different static model.

$$f(x) = m\,p(x) + n \qquad (4)$$

Due to the asymptotic tendencies of MET models, when $x \to 1$ ($\%MVC \to 100$), $f(x) \to 0$ and $p(x) \to 0$ ($MET \to 0$), we assume $n = 0$. Since some MET models are not suitable for $\%MVC \leq 15\%$, the regression is carried out from $x = 0.16$ to $x = 0.99$. With a step length 0.01, $N = 84$ MET values are calculated to determine the parameter m of each MET model by minimizing the function in Eq. 5.

$$M(x) = \sum_{i=1}^{N} (f(x_i) - m\,p(x_i))^2 = a\,m^2 + b\,m + c \qquad (5)$$

From Eq. 5, m can be calculated by Eq. 6.

$$m = \frac{-b}{2a} = \frac{\sum\limits_{i=1}^{N} p(x_i)f(x_i)}{\sum\limits_{i=1}^{N} p(x_i)^2} > 0 \qquad (6)$$

The regression result represents the fatigue resistance of the muscle group. In comparison with 6 general MET models, 6 elbow models, 5 shoulder models, and 6 hip/back models, different muscle fatigue resistances for corresponding muscle groups were calculated and listed below in Table 5. The mean value $\bar{m}$ and σ_m can be used to adjust our MET model to cover different MET models, and they can be further used to predict the fatigue resistance of a muscle group for a given population. The prediction with mean value and its deviation in general MET models is shown in Fig.6. It is observable that the bold solid curve and two slim solid curves cover most of the area formed by the previous empirical MET models.

It should be noted that the fatigue resistance for different muscle groups are only regressed based on the empirical data grouped in the literature, and the results (Table 6) for

shoulder and hip/back muscle groups did not conform to the normal distribution. For the shoulder joint, the subjects in these models were not only from different careers but also from different gender mixture. Therefore, the fatigue resistance result can only provide a reference in this study.

Table 5 Fatigue resistance $\bar{m}$ for different muscle groups

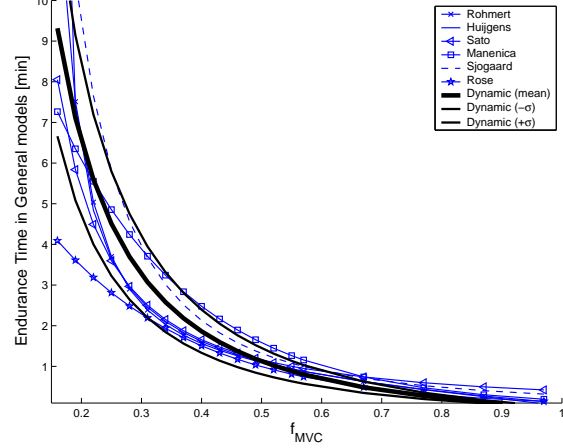| Segment	$\bar{m}$	σ_m
General	0.8135	0.2320
Shoulder	0.7562	0.4347
Elbow	0.8609	0.4079
Hip	1.9701	1.1476

Fig. 6 Prediction of MET in the dynamic MET model in comparison with that in the general models

Table 6 Fatigue resistances of shoulder MET models

Model	Subjects	m
Sato et al (1984)	5 male	0.427
Rohmert et al (1986)	6 male and 1 female students	0.545
Mathiassen and Ahsberg (1999)	20 male and 20 female municipal employees	0.698
Garg et al (2002)	12 female college subjects	1.393

4.3 Workflow for fatigue analysis

The general process of the posture analysis has been discussed in Section 3, and here is the flowchart in Fig. 7 to depict all the details in processing all the input information.

First, human motion obtained either from human simulation or from motion capture system is further processed to displacement $\mathbf{q}$, speed $\dot{\mathbf{q}}$, and acceleration $\ddot{\mathbf{q}}$ in general coordinates.
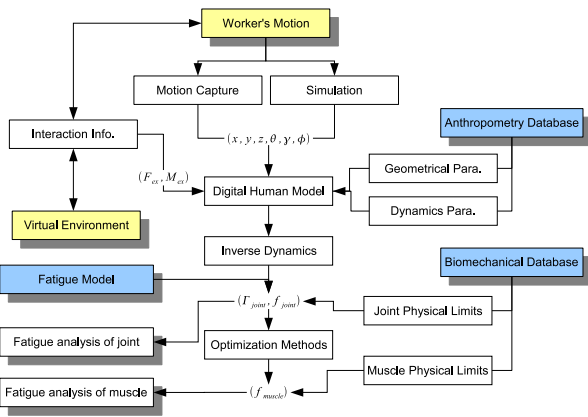
Fig. 7 Workflow for the fatigue evaluation

The external forces and torques on the human body are either measured directly by force measurement instruments or estimated in the simulation. The external loads are transformed to Γ_i and F_i in the coordinates attached to q_i in the modified DH method.

Human motion and interaction (forces, torques) are mapped into the digital human model which is geometrically and dynamically modeled from anthropometry database and the biomechanical database. Inverse dynamics is used to calculate the torque and force at each general joint. If it goes further, the effort of each individual muscle can be determined using optimization method as well.

Once the loads of the joints are determined, the fatigue of each joint can be analyzed using the fatigue model. The reduction of the physical strength can be evaluated, and finally the difficulty of the operation can be estimated by the change of physical strengths.

5 Analysis Results for EADS Application Cases - Drilling

5.1 Operation description

The application case is the assembly of two fuselage sections with rivets from the assembly line of an airplane in European Aeronautic Defence & Space (EADS) Company. One part of the job consists of drilling holes all around the cross section. The tasks is to drill holes around the fuselage circumference. The number of the holes could be up to 2,000 on an orbital fuselage junction of an airplane. The drilling machine has a weight around 5 kg, and even up to 7 kg in the worst condition with consideration of the pipe weight. The drilling force applied to the drilling machine is around 49N. In general, it takes 30 seconds to finish a hole. The drilling operation is illustrated in Fig. 8. The fatigue happens often in shoulder, elbow, and lower back because of the heavy load. Only the upper limb is taken into consider-

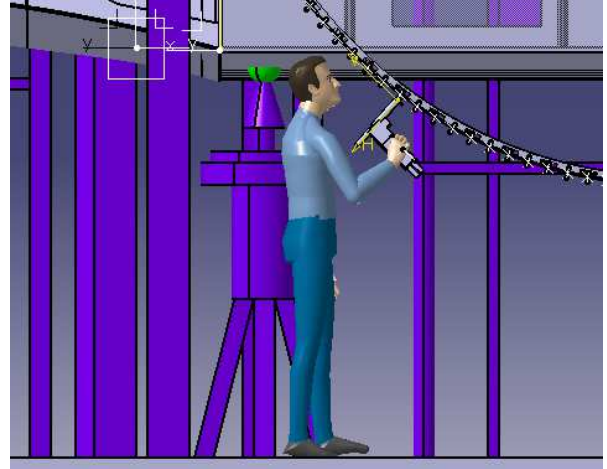ation in this demonstration case to decrease the complexity of the analysis.

Fig. 8 Drilling case in CATIA

5.2 Endurance time prediction

The drilling machine with a weight 5 kg is taken to calculate the maximum endurance time under a static posture with shoulder flexion as $30°$ and elbow flexion $90°$ for maintaining the operation in a continuous way. The weight of the drilling machine is divided by two in order to simplify the load sharing problem. The endurance result is shown in Table 7 for the population falling in the 95% strength distribution. It is found that the limitation of the work is determined by the shoulder, since the endurance time for the shoulder joint is much shorter than that of the elbow joint.

Table 7 Maximum endurance time of shoulder and elbow joints for drilling work

MET [sec]	$S - 2\sigma$	$S - \sigma$	S	$S + \sigma$	$S + 2\sigma$
Shoulder					
$\bar{m} - \sigma_m$	19.34	45.05	75.226	108.81	145.16
$\bar{m}$	45.489	105.96	176.94	255.94	341.44
$\bar{m} + \sigma_m$	71.639	166.87	278.65	403.07	537.71
Elbow					
$\bar{m} - \sigma_m$	230.61	424.27	640.47	873.52	1120.1
$\bar{m}$	438.27	806.3	1217.2	1660.1	2128.6
$\bar{m} + \sigma_m$	645.92	1188.3	1793.9	2446.6	3137.2

The difference in endurance results has two origins. One is the external load relative to the joint strength. The second comes from the fatigue resistance difference among the population. These differences are graphically presented from

Fig. 9 to Fig. 12. Figure 9 and Figure 10 show the variable endurance caused by the joint strength distribution in the adult male population with the mean fatigue resistance. Larger strength results in longer endurance time for the same external load. Figure 11 and Figure 12 present the endurance time for the population with the average joint strength but different fatigue resistances, and it shows that larger fatigue resistance leads to longer endurance time. Combining with the strength distribution and the fatigue resistance variance, the MET can be estimated for all the population.
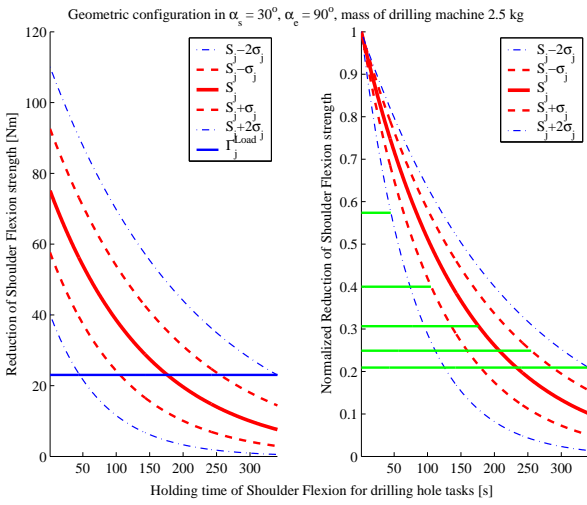

Fig. 11 Endurance time for the population with average strength for shoulder joint
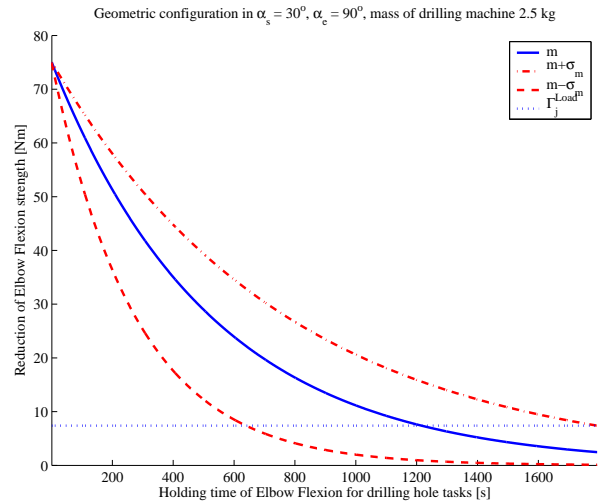
Fig. 12 Endurance time for the population with average strength for elbow joint

Fig. 9 Endurance time prediction for shoulder with average fatigue resistance

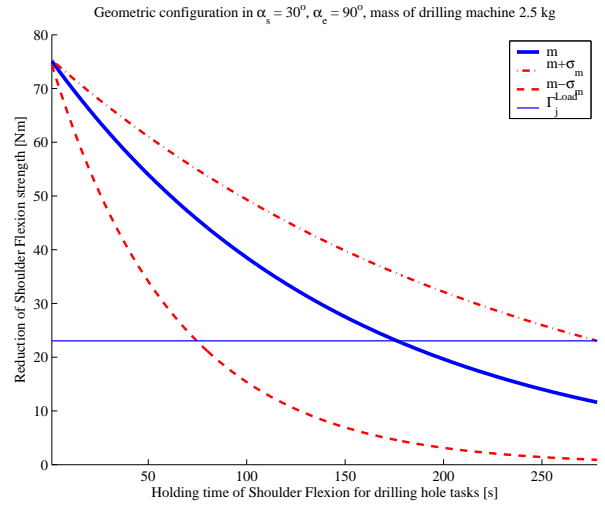**Fig. 10** Endurance time prediction for the elbow with average fatigue resistance

5.3 Fatigue evaluation

The fatigue is evaluated by the change of the joint strength in a fatigue operation. The working history can generate influence on the fatigue. Therefore, the fatigue for drilling a hole is evaluated in a continuous working process up to 6 holes. Only the population with the average strength and the average fatigue resistance is analyzed in fatigue evaluation in order to present the effect of the work history. The reduced strength is normalized by dividing the maximum joint strength, and it is shown in Fig. 13. It takes 30 seconds to drill a hole, and the joint strength is calculated and normalized every 30 seconds until exhaustion for the shoulder joint.

In our current research, **HS** includes only the joint strength vector. The evaluation of the fatigue is measured by the change
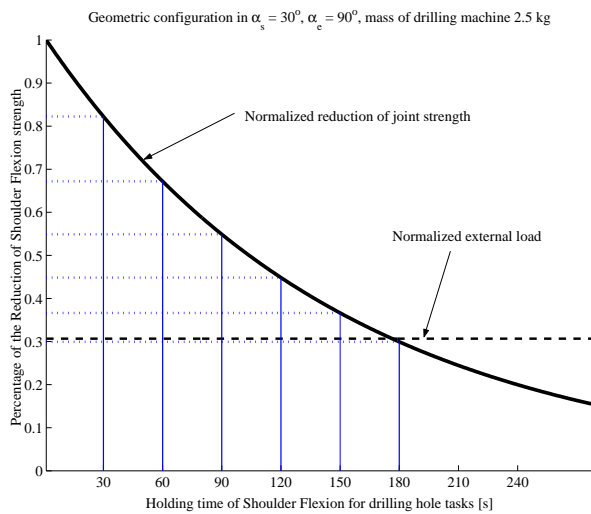
Fig. 13 Fatigue evaluation after drilling a hole in a continuous drilling process

of the joint strength for drilling a hole. The result is shown in Table 8. Three measurements are given in this table: one is the normalized physical strength every 30 seconds, noted as $\dfrac{\mathbf{HS}_i}{\mathbf{HS}_{max}}$; one is the difference between the joint strength before and after finishing a hole, noted as $\dfrac{\mathbf{HS}_i - \mathbf{HS}_{i+1}}{\mathbf{HS}_{max}}$; the last one if the difference between the joint strength and the maximum joint strength, noted as $\dfrac{\mathbf{HS}_{max} - \mathbf{HS}_i}{\mathbf{HS}_{max}}$. In Table 8, only the reduction of the shoulder joint strength is presented, since the relative load in elbow joint is much smaller.

From Fig. 13 and Table 8, the joint strength keeps the trend of descending in the continuous work. The ratio of the reduction gets smaller in the work progress due to the physiological change in the muscle fiber composition. More time consumed to work leads more reduction in physical strengths. The reduction relative to the maximum strength is able to assess the difficulty of the operations.

5.4 Experiment validation

Simulated drilling operations were tested under laboratory conditions in Tsinghua University. A total of 40 male industrial workers were asked to simulate the drilling work in a continuous operation for 180 seconds. Maximum output strengths were measured in the simulated operations at different periods of the operation. Fatigue was indexed by the reduction of the joint strength along time relative to the initial maximum joint strength. Three out of the 40 subjects could not sustain the external load for a duration of 180 seconds, and 34 subjects had a shoulder joint fatigue resistance (Mean=1.32, SD=0.62) greater than the average shoulder joint fatigue resistance in Table 5, which means that the

sample population has a higher fatigue resistance than the population grouped in the regression.

The physical strength has been measured in simulated job static strengths, and the reduction in the operation varies from 32.0% to 71.1% (Mean=53.7% and SD=9.1%). The reduction falls in the fatigue prediction of the theoretical methods in Table 9 (Mean=51.7%, SD=12.1%).

Table 9 Normalized torque strength reduction for the population with higher fatigue resistance

$\dfrac{\mathbf{HS}_{max} - \mathbf{HS}_{180}}{\mathbf{HS}_{max}}$	$S - 2\sigma$	$S - \sigma$	S	$S + \sigma$	$S + 2\sigma$
$\bar{m}$	-	-	69.9%	62.5%	56.3%
$\bar{m} + \sigma_m$	-	63.2%	53.2%	46.4%	40.8%
$\bar{m} + 2\sigma_m$	64.9%	51.9%	43.0%	36.7%	31.9%

5.5 Discussion

Under the proposed framework, the conception of the virtual human status is introduced and realized by a virtual human modeling and simulation tool. The virtual human is kinematic modeled based on the modeling method in robotics. Inverse dynamics is used to determine the joint loads. With the integration of a general fatigue model, the physical fatigue in a manual handling operation in EADS is simulated and analyzed. The decrease in human joint strengths can be predicted in the theoretical approach, and it has been validated with experimental data.

Human status is introduced in this framework in order to generalize all the discussion for the human simulation. We concentrate only on the physical aspect of the virtual human, in particular on joint strengths. Physical status can be extended to other aspects, either measurable using instruments (e.g., heart rate, oxygen consumption, electromyograph of muscle, etc.) or predicable using mathematical models (e.g., vision, strength, etc.). Similarly, the mental status of human can also be established by similar terms (e.g., mental capacity, mental workload, mental fatigue, etc.). Under the conception of human status, different aspects of the human can be aggregated together to present the virtual human completely. The changed human status caused by a physical job or a mental job can be measured or predicted to assess different aspects of the job. It should be noted that the definition of human status is still immature and it requires great effort to form, extend, and validate this conception.

The main difference between the fatigue analysis in our study and the previous methods for posture analysis is: in previous methods (Wood et al, 1997; Iridiastadi and Nussbaum, 2006; Roman-Liu et al, 2005), intermittent procedures were used to develop the fatigue model with job specific parameters; in contrast, all the related physical exposure factors

Table 8 Normalized shoulder joint strength in the drilling operation

Time [s]	0	30	60	90	120	150	180
$\bar{m}$							
$\dfrac{\mathbf{HS}_i}{\mathbf{HS}_{max}}$	100%	82.2%	67.2%	54.9%	44.8%	36.6%	30.1%
$\dfrac{\mathbf{HS}_i - \mathbf{HS}_{i+1}}{\mathbf{HS}_{max}}$	0%	17.8%	15.0%	12.3%	10.1%	8.2%	6.5%
$\dfrac{\mathbf{HS}_{max} - \mathbf{HS}_i}{\mathbf{HS}_{max}}$	0%	17.8%	32.8%	45.1%	55.2%	63.4%	69.9%

are taken into consideration in a continuous approach in our model. In this way, the analysis of the manual handling operation can be generalized without limitations of job specific parameters. Furthermore, the fatigue and recovery procedures can be decoupled to simplify the analysis in a continuous way. Although only a specific application case is presented in this paper, the feasibility of the general concept has been verified by the introduction of human status and the validation of the fatigue model.

It should be noted that the recovery of the physical strength has not been considered yet. Although there are several work-rest allowance models in the literature, substantial variability was found among the prediction results for industrial operations (El ahrache and Imbeau, 2009) and it is still ongoing to develop a general recovery model.

6 Conclusions

In this study, human status is introduced into the work evaluation system, especially for the physical status. It provides a global definition under which different aspects of human abilities can be integrated and assessed simultaneously. The effect of the work on the human status, either positive or negative, can be measured by the change of the human status before and after the operation. We concentrate our study on physical aspects, especially on joint moment strengths. The physical fatigue analysis in a drilling case under the work evaluation framework demonstrates the work flow and the functions of the virtual human simulation. The change of joint moment strength, a specific aspect of human physical status, has been simulated based on a general fatigue model with fatigue resistances. The similar results between the analysis and the experimental data suggests that the framework may be useful for assessing the physical status in continuous static operations.

The new conception human status and the theoretical method for assessing the physical status may provide a new approach to generalize the virtual human simulation and evaluate the physical aspect in continuous static manual handling operations. This approach is useful to assess the physical load to prevent industrial workers from MSD risks, and

it can also be used to assess mental load with extension of mental status.

However, it should be noted that great effort has to be done to extend different aspects in human status to make it more precise. Even only for physical fatigue, it is still necessary to develop a recovery model to complete the fatigue prediction.

References

Anderson D, Madigan M, Nussbaum M (2007) Maximum voluntary joint torque as a function of joint angle and angular velocity: Model development and application to the lower limb. Journal of Biomechanics 40(14):3105–3113

Badler NI, Phillips GB, Webber BL (1993) Simulating humans: computer graphics animation and control. Oxford University Press, USA

Bubb H, Engstler F, Fritzsche F, Mergl C, Sabbah O, Schaefer P, Zacher I (2006) The development of RAMSIS in past and future as an example for the cooperation between industry and university. International Journal of Human Factors Modelling and Simulation 1(1):140–157

Chaffin D (2002) On simulating human reach motions for ergonomics analyses. Human Factors and Ergonomics in Manufacturing 12(3):235–247

Chaffin D (2007) Human motion simulation for vehicle and workplace design. Human Factors and Ergonomics in Manufacturing 17(5):475

Chaffin DB, Andersson GBJ, Martin BJ (1999) Occupational biomechanics, 3rd edn. Wiley-Interscience

Chedmail P, Chablat D, Roy CL (2003) A distributed approach for access and visibility task with a manikin and a robot in a virtual reality environment. IEEE Transactions on Industrial Electronics 50(4):692–698

Chen Y (2000) Changes in lifting dynamics after localized arm fatigue. International Journal of Industrial Ergonomics 25(6):611–619

Damsgaard M, Rasmussen J, Christensen S, Surma E, de Zee M (2006) Analysis of musculoskeletal systems in the AnyBody Modeling System. Simulation Modelling Practice and Theory 14(8):1100–1111

Ding J, Wexler AS, Binder-Macleod SA (2000) A predictive model of fatigue in human skeletal muscles. Journal of Applied Physiology 89:1322–1332

El ahrache K, Imbeau D (2009) Comparison of rest allowance models for static muscular work. International Journal of Industrial Ergonomics 39(1):73–80

El ahrache K, Imbeau D, Farbos B (2006) Percentile values for determining maximum endurance times for static muscular work. International Journal of Industrial Ergonomics 36(2):99–108

Fuller J, Lomond K, Fung J, Côté J (2008) Posture-movement changes following repetitive motion-induced shoulder muscle fatigue. Journal of electromyography and kinesiology: official journal of the International Society of Electrophysiological Kinesiology

Garg A, Hegmann K, Schwoerer B, Kapellusch J (2002) The effect of maximum voluntary contraction on endurance times for the shoulder girdle. International Journal of Industrial Ergonomics 30(2):103–113

Giat Y, Mizrahi J, Levy M (1993) A musculotendon model of the fatigue profiles of paralyzed quadriceps muscle under FES. IEEE Transactions on Biomechanical Engineering 40(7):664–674

Hill A (1938) The heat of shortening and the dynamic constants of muscle. Proceedings of the Royal Society of London Series B, Biological Sciences 126(843):136–195

Hou H, Sun S, Pan Y (2007) Research on virtual human in ergonomic simulation. Computers & Industrial Engineering 53(2):350–356

Iridiastadi H, Nussbaum M (2006) Muscle fatigue and endurance during repetitive intermittent static efforts: development of prediction models. Ergonomics 49(4):344–360

Khalil W, Dombre E (2002) Modelling, identification and control of robots. Hermes Science Publications

Komura T, Shinagawa Y, Kunii TL (2000) Creating and retargetting motion by the musculoskeletal human. The Visual Computer 16(5):254–270

Li G, Buckle P (1999) Current techniques for assessing physical exposure to work-related musculoskeletal risks, with emphasis on posture-based methods. Ergonomics 42(5):674–695

Liu J, Brown R, Yue G (2002) A dynamical model of muscle activation, fatigue, and recovery. Biophysical Journal 82(5):2344–2359

Ma L, Chablat D, Bennis F, Zhang W (2009) A new simple dynamic muscle fatigue model and its validation. International Journal of Industrial Ergonomics 39(1):211–220

Mathiassen S, Ahsberg E (1999) Prediction of shoulder flexion endurance from personal factor. International Journal of Industrial Ergonomics 24(3):315–329

Rohmert W, Wangenheim M, Mainzer J, Zipp P, Lesser W (1986) A study stressing the need for a static postural force model for work analysis. Ergonomics 29(10):1235–1249

Roman-Liu D, Tokarski T, Kowalewski R (2005) Decrease of force capabilities as an index of upper limb fatigue. Ergonomics 48(8):930–948

Sato H, Ohashi J, Iwanaga K, Yoshitake R, Shimada K (1984) Endurance time and fatigue in static contractions. Journal of human ergology 13(2):147–154

Tilley AR, Dreyfuss H (2002) The measure of man & woman. Human factors in design. Revised Edition. New York: John Wiley & Sons, Inc.

Vignes RM (2004) Modeling muscle fatigue in digital humans. Master's thesis, Graduate College of The University of Iowa

VSR Research Group (2004) Technical report for project virtual soldier research. Tech. rep., Center for Computer-Aided Design, The University of IOWA

Wood D, Fisher D, Andres R (1997) Minimizing fatigue during repetitive jobs: optimal work-rest schedules. Human Factors: The Journal of the Human Factors and Ergonomics Society 39(1):83–101

Xia T, Frey Law L (2008) A theoretical approach for modeling peripheral muscle fatigue and recovery. Journal of Biomechanics 41(14):3046–3052

Yang J, Pitarch E, Kim J, Abdel-Malek K (2006) Posture prediction and force/torque analysis for human hands. In: Proc. of SAE Digital human modelling for design and engineering conference, p 2326

Yang J, Sinokrot T, Abdel-Malek K (2008) A general analytic approach for Santos upper extremity workspace. Computers & Industrial Engineering 54(2):242–258

r = 0.7254
y = 0.6264x+0.0360

Task performances in virtual environment